



Cite this: *Photochem. Photobiol. Sci.*, 2016, **15**, 920

Heterodimerization at the dye sensitized TiO₂ surface: an efficient strategy toward quick removal of water contaminants

Zaki S. Seddigi,^a Saleh A. Ahmed,^{*b} Samim Sardar^c and Samir Kumar Pal^{*c}

Sensitization of wide bandgap semiconductors with heterodimers for better solar light sensitivity has attracted widespread attention in the recent times. However, application of heterodimerization for removing soluble water pollutants from waste water is sparse in the literature. In the present study, we have utilized heterodimerization of a model pollutant methylene blue (MB) with a ruthenium based dye N719 for the removal of the pollutant. We have synthesized N719 functionalized carbonate doped TiO₂ microspheres (doped MS) which act as a novel material for the detoxification of MB containing water by adsorbing at the surface and eventually killing by photoinduced reduction under visible light irradiation. The mechanism of surface adsorption and photoreduction of MB are explored using steady state and time resolved spectroscopy studies. We have fabricated two types of prototype devices (flow device and active filter) using the functionalized doped MS. Both the devices show excellent dye removal activity and recyclability. The present study would find relevance in the removal of soluble pollutants from waste water.

Received 12th March 2016,

Accepted 2nd June 2016

DOI: 10.1039/c6pp00071a

www.rsc.org/pps

Introduction

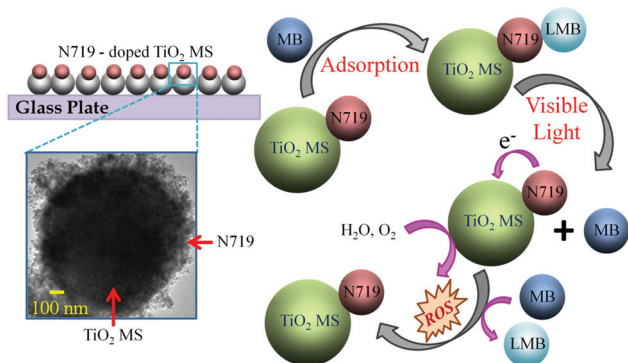
Photosensitization of wide bandgap light harvesting semiconductors (TiO₂, ZnO) with organic dyes for their use in visible light photocatalysis (VLP) and dye-sensitized solar cells (DSSC) is well documented in the literature.^{1–7} However, the use of homo- and heterodimers of organic molecules for the sensitization of light harvesting semiconductors for better solar light sensitivity is a relatively new strategy, which was started early in this century.^{8–12} In one of the earlier studies, monolayers of oriented covalently linked zinc/free base porphyrin heterodimers onto ~30 nm nonporous layers of TiO₂ exhibit increased photocurrent yield. The heterodimers act as light harvesting antennae where the antenna molecule in the dimer contributes to the photocurrent through the transfer of excitation energy to the surface bonded moiety.⁹ In another study, singlet–singlet energy transfer from the zinc or free-base porphyrin to phthalocyanine on the TiO₂ surface has been employed as wide-band capturing solar energy harvesting

materials in photoelectrochemical cells.⁸ The combination of porphyrin and ruthenium–polypyridyl complexes as supra-molecular sensitizers to the wide bandgap semiconductor leads to versatile molecular interfaces and improved photo-response efficiency.¹³ In a recent effort from us, we have used tartrate-zinc phthalocyanine covalently linked heterodimers onto an ~30 nm nonporous layer of ZnO for efficient VLP near the red region of the solar spectrum.¹⁴ In the heterodimers the carboxyl group of the tartrate was responsible for attaching the dimer to ZnO and making a link to the central Zn metal of the phthalocyanine. The phthalocyanine moiety was solely responsible for light absorption and eventually photoinduced charge separation. Mártire *et al.* have shown the reactivity of dichlorophen sorbed on silica nanoparticles with the excited states of riboflavin, a sensitizer usually present in natural waters, and with singlet oxygen.¹⁵ P. Ciambelli *et al.* have shown the removal of spiramycin in the presence of N-doped TiO₂ suspension under visible light irradiation.¹⁶ In the present study, we have sensitized mesoporous carbonate doped TiO₂ microspheres (doped MS) with the well-known ruthenium based dye N719 (Scheme 1). A detailed structural characterization using optical spectroscopy and electron microscopy reveals more efficient attachment of N719 to the doped MS surface compared to its undoped counterpart leading to higher dye loading in the doped MS. We have shown that N719 in bulk solvent makes efficient heterodimers with methylene blue (MB), one of the model water pollutants from textile indus-

^aDepartment of Environmental Health, Faculty of Public Health and Health Informatics, Umm Al-Qura University, 21955 Makkah, Saudi Arabia

^bChemistry Department, Faculty of Applied Sciences, Umm Al-Qura University, 21955 Makkah, Saudi Arabia. E-mail: skpal@bose.res.in, saleh_63@hotmail.com

^cDepartment of Chemical, Biological and Macromolecular Sciences, S. N. Bose National Centre for Basic Sciences, Block JD, Sector III, Salt Lake, Kolkata 700 098, India



Scheme 1 The N719 functionalized doped TiO_2 MS thin film on a glass plate and the inset shows the TEM image of the functional material. The right panel shows the mechanistic pathways of the methylene blue (MB) adsorption on the surface of the functional material and the photo-induced reduction of MB to leuco methylene blue (LMB) through the formation of reactive oxygen species (ROS) under visible light irradiation.

tries.¹⁷ The heterodimerization of MB with N719 is more effective in the monomeric form of the pollutant than in the dimeric form leading to static fluorescence quenching of MB in bulk solvent as revealed from picosecond resolved fluorescence spectroscopy. Our studies show that N719 functionalized doped MS as a novel material for the detoxification of MB containing water by adsorbing at the surface and eventually killing by photoinduced reduction. The mechanism of surface adsorption and photoreduction of MB are also explored in the present study.

Materials and methods

Reagents

Titanium isopropoxide, urea, thiourea, di-tetrabutylammonium *cis*-bis(isothiocyanato)bis(2,2'-bipyridyl-4,4'-dicarboxylato)ruthenium(II) (N719), and methylene blue were purchased from Sigma-Aldrich. Ultrapure water (Millipore System, 18.2 M Ω cm), ethanol and acetone (purchased from Merck) were used as solvents. Analytical-grade chemicals were used for synthesis without further purifications.

Synthesis of TiO_2 microspheres and carbonate doped TiO_2 microspheres

The mesoporous TiO_2 microspheres were synthesized by following the modified previously reported literature.^{18,19} In brief, 1 mL of titanium isopropoxide was mixed with 15 mL of anhydrous acetone and then stirred for 15 min. Then the solution was transferred into a 20 mL Teflon lined stainless-steel autoclave and heated at 180 °C for 12 h. The precipitate was collected and washed with acetone and then with ethanol several times. The sample was dried at 60 °C. Carbonate doped TiO_2 MS were synthesized by mixing the synthesized TiO_2 MS, urea and thiourea (1 gm, 1.5 gm and 2 gm, respectively). The mixture was ground for 20 min and then annealed at 400 °C

for 5 h. After annealing the powder was washed with water several times and then dried at 60 °C.

Synthesis of N719 sensitized TiO_2 MS and doped TiO_2 MS samples

0.5 mM N719 solution was prepared in ethanol under constant stirring for 1 h. The sensitization of TiO_2 MS and doped TiO_2 MS with the N719 dye was carried out at room temperature in the dark by adding TiO_2 MS and doped TiO_2 MS into a 0.5 mM dye solution with continuous stirring for 12 h. After the sensitization process, the solution was centrifuged for a few minutes and the clear supernatant solution of the unattached dyes was removed. Then the sensitized material was washed with ethanol several times to remove any unattached dye. The nano-hybrid was then dried in a water bath and stored in the dark until further use.

Characterization methods

Field Emission Scanning Electron Microscopy (FESEM, QUANTA FEG 250) was used to investigate the surface morphology of the samples. Transmission electron microscopy (TEM) was carried out using an FEI (Technai S-Twin) instrument with an acceleration voltage of 200 kV. The MS samples were taken in ethanol and stirred for few minutes. Then, a drop of the sample was placed on a carbon-coated copper grid and dried at room temperature. The particle sizes were determined from micrographs recorded at a high magnification of 100 000 \times . For optical experiments, the steady-state absorption and emission spectra were recorded with a Shimadzu UV-2600 spectrophotometer and with a Jobin Yvon Fluoromax-3 fluorimeter, respectively. Picosecond resolution spectroscopy studies were carried out using a commercial time correlated single photon counting (TCSPC) setup from Edinburgh Instruments (instrument response function, IRF = 80 ps, excitation at 633 nm). The details of the experimental setup and methodology were described in our earlier report.^{20–22}

Photocatalytic tests

The photocatalytic activity of the nano-hybrid under visible light illumination has been tested for photodecomposition of methylene blue (MB, taken as a model pollutant) in water. The photodegradation reaction of MB (initial concentration $C_0 = 6 \times 10^{-6}$ M) was carried out in a 10 mm optical path quartz cell reactor containing 3.5 mL of a model solution with a concentration of 0.1 g L⁻¹ of the nano-hybrid. The suspension was irradiated with a white LED (50 W) and absorption spectra were collected at different time intervals. There was no increase in temperature of the quartz cell reactor upon light irradiation within the experimental time window. A magnetic stirrer was used to maintain the suspension of the photocatalyst in the solution. The percentage degradation (%DE) of MB was determined using eqn (1):

$$\%DE = \frac{I_0 - I}{I_0} \times 100 \quad (1)$$

where I_0 is the initial absorbance of MB at $\lambda_{\max} = 664$ nm and I is the absorbance of MB after light irradiation.

Langmuir–Hinshelwood (L-H) kinetic model

The Langmuir–Hinshelwood equation can describe the dependence of [MB] on the degradation rates:^{23,24}

$$R_0 = \frac{dC}{dt} = \frac{k_{L-H}KC_0}{1 + KC_0} \quad (2)$$

where, C_0 is the initial concentration of the MB solution, t is the irradiation time, k_{L-H} is the Langmuir–Hinshelwood rate constant, and K is the Langmuir adsorption coefficient of the MB molecules. At a lower initial concentration of MB ($KC_0 \ll 1$), eqn (2) can be simplified to an apparent first order equation:

$$R_0 = k_{L-H}KC_0 = k_{app}C_0 \quad (3)$$

where, k_{app} is the apparent first-order rate constant. If the initial concentration of MB is sufficiently high ($KC_0 \gg 1$), eqn (2) can be simplified to a zero order rate equation:

$$R_0 = k_{L-H} \quad (4)$$

Results and discussion

Fig. 1a shows the scanning electron microscopy (SEM) images of the synthesized doped TiO_2 MS with a diameter of $\sim 1 \mu\text{m}$. The microsphere is composed of densely packed TiO_2 nanocrystals as shown in Fig. 1b. The detailed characterization of the TiO_2 MS and doped TiO_2 MS has been published elsewhere.²⁵ For the prototype devices, two types of thin films were prepared. Fig. 1c shows an SEM image of the thin film prepared on a glass slide to make the flow device. The SEM image of the doped MS loaded polymeric membrane for another prototype of water decontamination is also shown in Fig. 1d. The bare polymeric membrane with a pore size of ~ 220 nm is shown in the inset of Fig. 1d. Extremely efficient MB adsorption kinetics on the functionalized doped MS compared to other materials as controls are shown in Fig. 2a. The TiO_2 MS and doped TiO_2 MS samples show MB adsorption ($\sim 15\%$) due to the porosity in the microspheres. The N719 functionalized samples exhibit very rapid adsorption kinetics. The N719 functionalized doped MS shows faster adsorption kinetics than that of the undoped counterpart due to more N719 dye loading on the doped MS surface. The carbonate doping in TiO_2 MS increases the porosity which is responsible for enhanced dye loading as shown in our earlier publication.²⁵

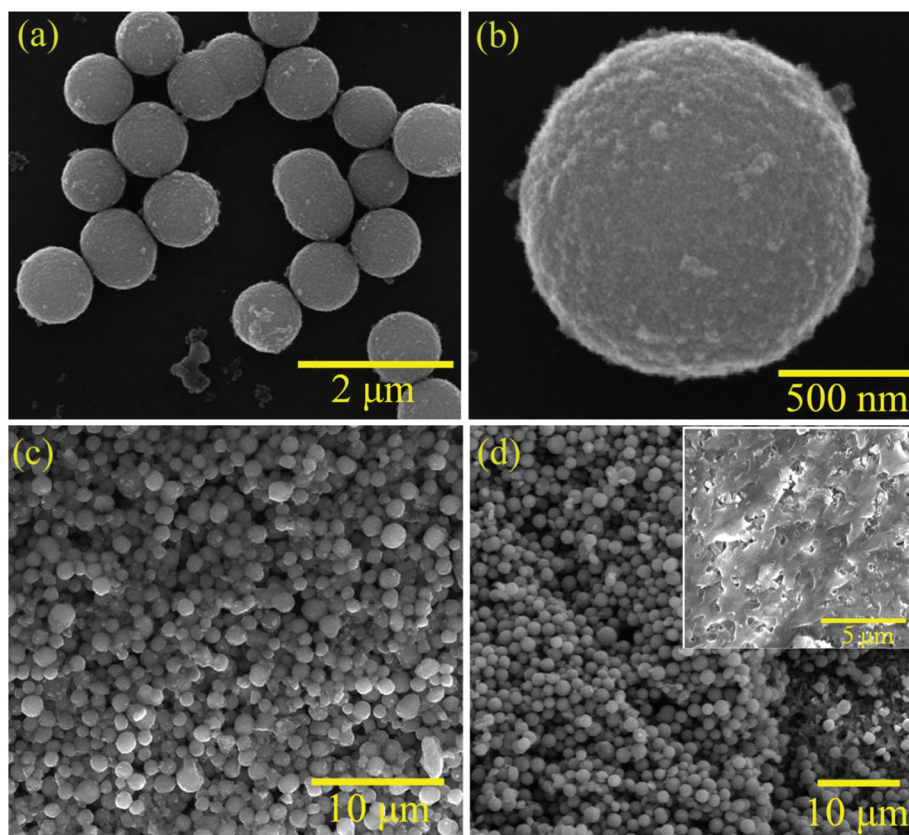


Fig. 1 SEM images of (a, b) doped TiO_2 MS, (c) the thin film of doped TiO_2 MS on the glass slide, (d) doped TiO_2 MS embedded on the polymer membrane; the inset shows the bare polymer membrane.

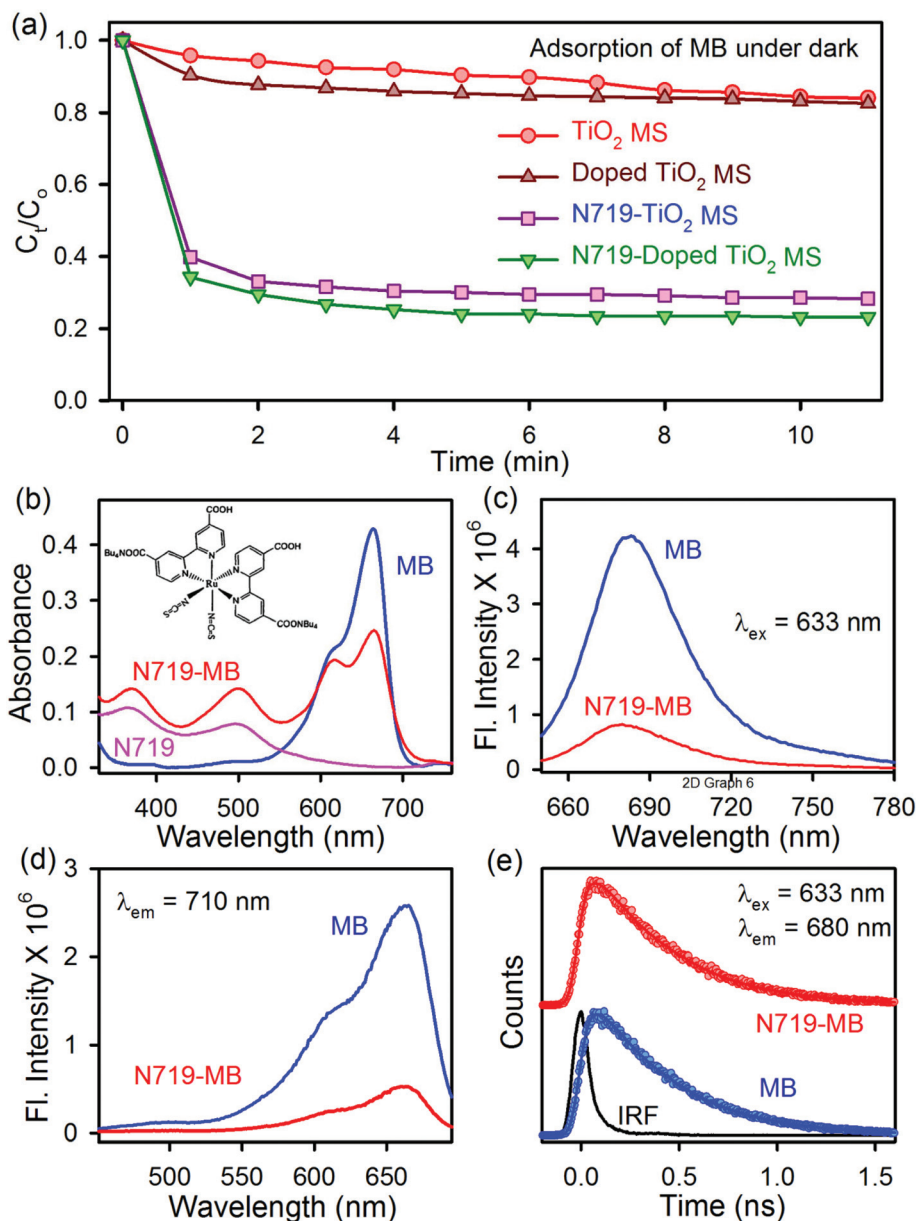


Fig. 2 (a) Adsorption of MB on N719 functionalized doped TiO₂ MS and other control materials under dark conditions. (b) Heterodimerization of MB with N719 in water from absorption spectra. The inset shows the chemical structure of the N719 dye. (c) Emission and (d) excitation spectra of MB in the presence and absence of N719. (e) Picosecond resolved fluorescence transients of MB and MB-N719 heterodimer.

In order to investigate the interaction between N719 and MB, the optical spectroscopy measurements were performed in the bulk solvent. Evidence of heterodimerization of N719 with MB in the bulk solvent is shown in Fig. 2b–d. The complexation of N719 with the monomeric form of MB through a nonfluorescence charge transfer MB-complex is consistent with earlier studies²⁶ as shown in Fig. 2b.

The positively charged MB forms heterodimers with the negatively charged groups present in the N719 due to the electrostatic interaction.²⁶ The quenching in the emission and excitation spectra of MB due to the formation of the charge transfer complex (N719-MB) is shown in Fig. 2c and d, respec-

tively. To investigate the nature of the quenching, picosecond resolved fluorescence studies were performed and the results are shown in Fig. 2e. The lifetime of MB remains unaltered after the N719-MB complex formation which reveals the static nature of the quenching. In order to study the nature of surface adsorption of MB on the N719 functionalized doped TiO₂ MS, the adsorption kinetics were monitored as a function of the MB concentration as shown in Fig. 3a. Initially the adsorption rate increases with an increase in the MB concentration, however the rate remains constant after a certain concentration of MB. The R_0 versus C_0 curve is fitted well using the Langmuir–Hinshelwood equation (eqn (2)) as shown in

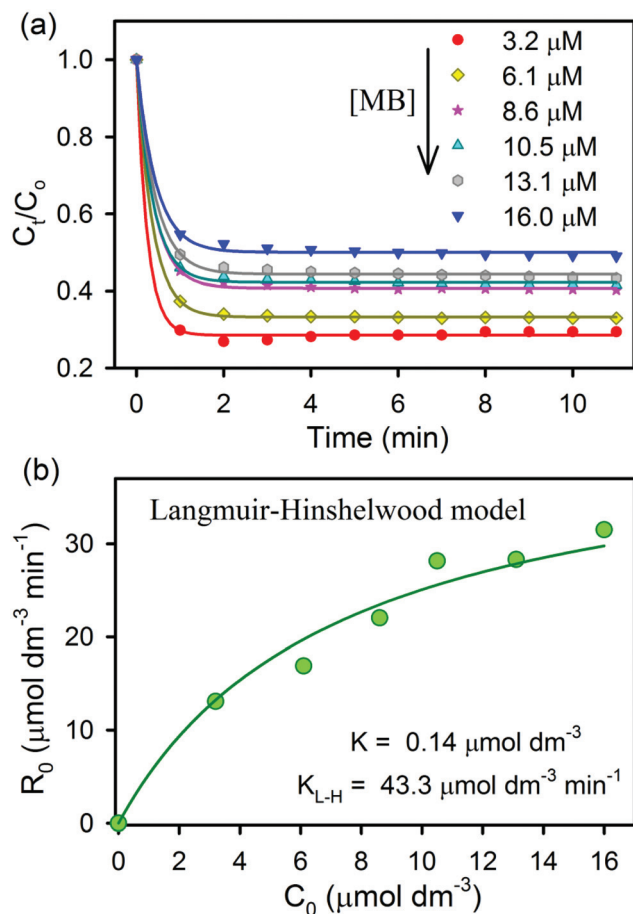


Fig. 3 (a) MB adsorption kinetics on N719 functionalized doped TiO_2 MS with various MB concentrations. (b) Degradation rate (R_0) versus initial MB concentration (C_0) plot.

Fig. 3b. The Langmuir adsorption coefficient (K) and the Langmuir-Hinshelwood rate constant (k_{L-H}) of MB molecules are found to be $0.14 \mu\text{mol dm}^{-3}$ and $43.3 \mu\text{mol dm}^{-3} \text{min}^{-1}$, respectively.

The effect of light exposure on the heterodimers at the doped MS surface is evident from Fig. 4a. An increase in MB in the presence of white light (more in doped MS and less in N719 alone) could be due to the regeneration of MB from instantly reduced LMB at the surface of doped MS upto ~ 70 min. Upon further light irradiation, the MB in the solution of N719 alone remains unaffected. However, the MB in the presence of N719 functionalized doped MS degrades completely in 180 min. The N719 upon excitation with visible light injects electrons to the TiO_2 conduction band (CB). The CB electrons react with dissolved oxygen present in the solution to form reactive oxygen species and eventually lead to the reduction of MB to its leuco form.^{27,28} The photocatalytic activity of the doped TiO_2 MS alone was also investigated under white light irradiation ($\lambda > 450$ nm) and found only 10% MB degradation in 150 min under our experimental conditions. The absorption spectra of MB in the supernatant at

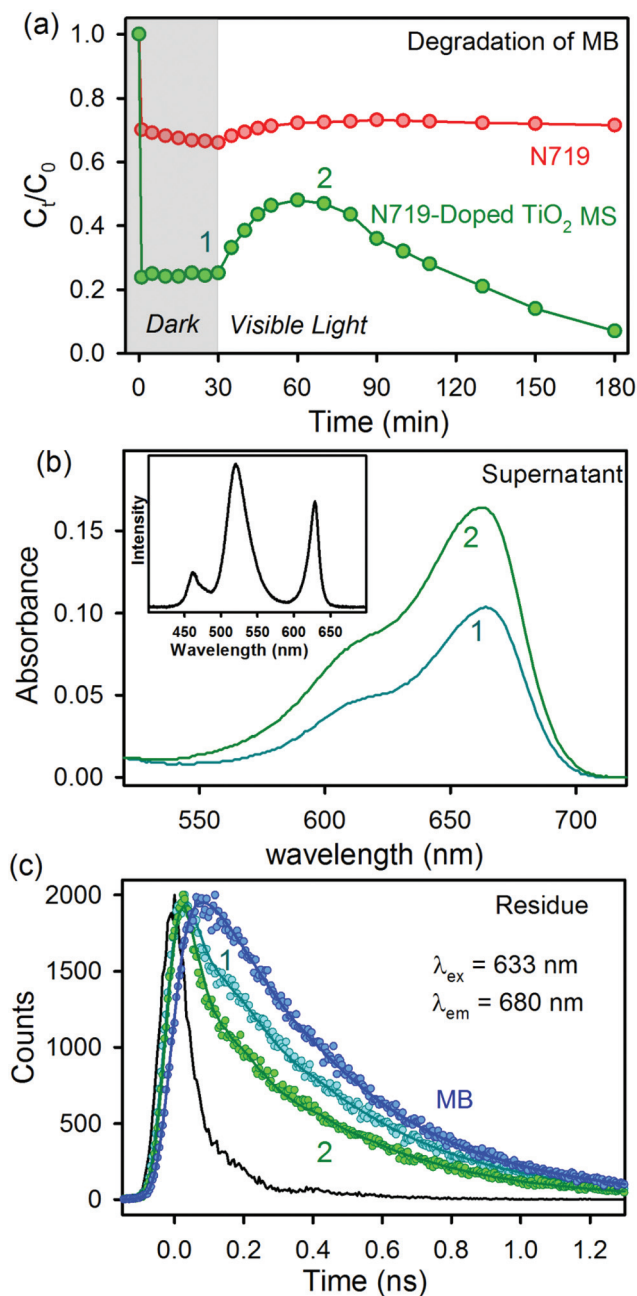


Fig. 4 (a) Degradation of MB in the dark and then white light irradiation in the presence of N719 functionalized doped TiO_2 MS and N719 alone. (b) Absorption spectra of MB in the supernatant at position 1 and 2. Inset shows the emission spectrum of the LED used as the light source for the photocatalysis experiment. (c) Picosecond resolved fluorescence transients of MB and the residues at position 1 and 2.

different time intervals of light irradiation are shown in Fig. 4b. The absorbance of the supernatant at position 2 shows the presence of more MB in the solution than that at position 1. However in the residue, the pollutant MB shows a faster fluorescence decay (20 ps (77%)) at position 1 compared to MB alone in bulk solvent (380 ps). At position 2 the fluorescence decay becomes faster (20 ps (86%)) revealing tightly adsorbed

Table 1 Dynamics of picosecond-resolved luminescence transients^a

Sample	τ_1 (ps)	τ_2 (ps)	τ_{av} (ps)
MB	380 (100%)	—	380
MB-N719	380 (100%)	—	380
Residue at position 1	20 (77%)	380 (23%)	102.8
Residue at position 2	20 (86%)	380 (14%)	70.4

^a Numbers in parentheses indicate relative weightages. The excitation wavelength was at 633 nm and emission monitored at 680 nm.

MB which are undergoing efficient photoinduced electron transfer to the sensitized doped MS. The details of the spectroscopy parameters and the fitting parameters of the fluo-

rescence decays are tabulated in Table 1. The overall mechanism is shown in Scheme 1.

After the synthesis, thorough characterization of the functional doped MS and confirmation of the efficacy of soluble dye removal, we have made a prototype flow device as shown in Fig. 5a. The prototype flow device exhibits excellent dye removal activity (data not shown). Fig. 5b shows another prototype device using functional doped MS embedded on the polymeric membrane as an activated filter. The activated filter instantly adsorbed the soluble pollutant (MB) from waste water and then upon photoirradiation the functional material can be regenerated. The images of the activated filter during different experimental time intervals are shown in Fig. 5c. The

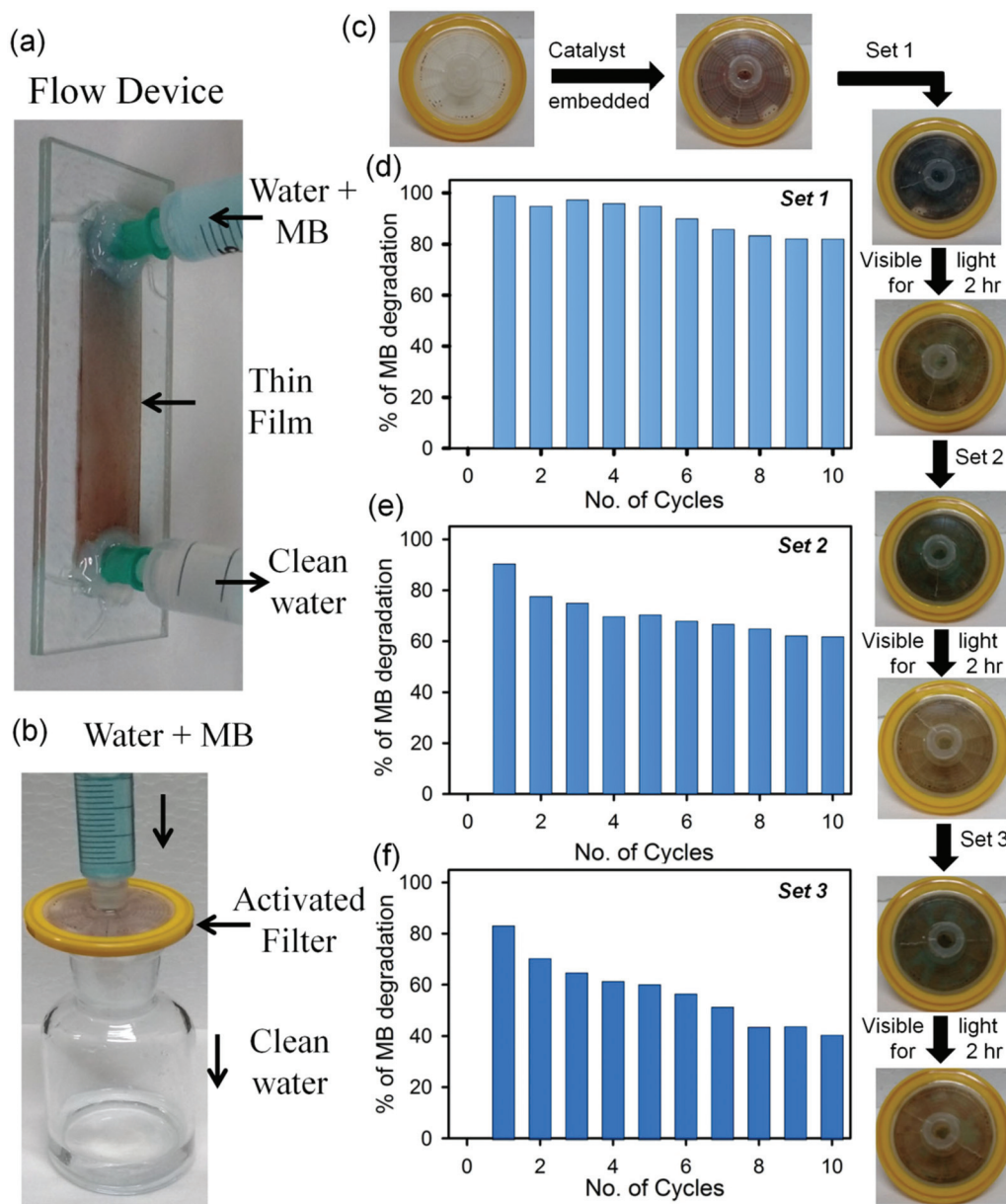


Fig. 5 Images of the prototype devices, (a) the flow device and (b) the activated filter. (c) Images of the activated filter at different intervals. MB degradation using the activated filter in different sets (d–f).

dye removal activity and recyclability of the activated filter were checked for three sets as shown in Fig. 5(d-f). 2 mg of the functional material were embedded on the polymeric membrane and 10 cycles were performed in each set with 2 mL of 6×10^{-6} M aqueous MB solutions in each cycle. After each set, the filter was cleaned by using visible light irradiation for 2 hours. The experimental results suggest excellent adsorption and recyclability of the prototype devices. As ruthenium based dyes are expensive, we will focus on the development of less expensive dyes in our future projects in order to make low cost devices using this concept.

Conclusion

In summary, we have demonstrated that N719 functionalized mesoporous doped MS can be used as functional materials for removing soluble model water pollutants from textile industries. The mechanism of dye removal through efficient heterodimerization at the doped MS surface is also established. The heterodimerization of MB with N719 is more effective in the monomeric form of the pollutant rather than the dimeric form. The efficient photoreduction of the adsorbed dye under visible light irradiation revealing excellent recyclability of the material is also demonstrated. We have used the material in two varieties of prototypes (active filter and flow device) for the potential use of the material in real field. Both the prototype devices exhibit excellent dye removal activity and recyclability. The present study provides a simple and an economic way to design functional materials and prototype devices for cleaning soluble organic pollutants from waste water.

Acknowledgements

The authors wish to acknowledge the support of King Abdul Aziz City for Science and Technology (KACST) through the Science & Technology Unit at Umm Al-Qura University for funding through Project No. 12-NANO2317-10 as part of the National Science, Technology and Innovation Plan.

References

- 1 W. J. Youngblood, S.-H. A. Lee, K. Maeda and T. E. Mallouk, Visible Light Water Splitting Using Dye-Sensitized Oxide Semiconductors, *Acc. Chem. Res.*, 2009, **42**, 1966–1973.
- 2 M. Gratzel, Photoelectrochemical cells, *Nature*, 2001, **414**, 338–344.
- 3 S. Sardar, S. Sarkar, M. T. Z. Myint, S. Al-Harathi, J. Dutta and S. K. Pal, Role of central metal ions in hematoporphyrin-functionalized titania in solar energy conversion dynamics, *Phys. Chem. Chem. Phys.*, 2013, **15**, 18562–18570.
- 4 B. E. Hardin, H. J. Snaith and M. D. McGehee, The renaissance of dye-sensitized solar cells, *Nat. Photonics*, 2012, **6**, 162–169.
- 5 S. Mathew, A. Yella, P. Gao, R. Humphry-Baker, F. E. Curchod-Basile, N. Ashari-Astani, I. Tavernelli, U. Rothlisberger, K. Nazeeruddin-Md and M. Grätzel, Dye-sensitized solar cells with 13% efficiency achieved through the molecular engineering of porphyrin sensitizers, *Nat. Chem.*, 2014, **6**, 242–247.
- 6 G. Qin, Y. Zhang, X. Ke, X. Tong, Z. Sun, M. Liang and S. Xue, Photocatalytic reduction of carbon dioxide to formic acid, formaldehyde, and methanol using dye-sensitized TiO₂ film, *Appl. Catal., B.*, 2013, **129**, 599–605.
- 7 M. Pelaez, N. T. Nolan, S. C. Pillai, M. K. Seery, P. Falaras, A. G. Kontos, P. S. M. Dunlop, J. W. J. Hamilton, J. A. Byrne, K. O'Shea, M. H. Entezari and D. D. Dionysiou, A review on the visible light active titanium dioxide photocatalysts for environmental applications, *Appl. Catal., B.*, 2012, **125**, 331–349.
- 8 C. B. Kc, K. Stranius, P. D'Souza, N. K. Subbaiyan, H. Lemmetyinen, N. V. Tkachenko and F. D'Souza, Sequential Photoinduced Energy and Electron Transfer Directed Improved Performance of the Supramolecular Solar Cell of a Zinc Porphyrin–Zinc Phthalocyanine Conjugate Modified TiO₂ Surface, *J. Phys. Chem. C*, 2013, **117**, 763–773.
- 9 R. B. M. Koehorst, G. K. Boschloo, T. J. Savenije, A. Goossens and T. J. Schaafsma, Spectral Sensitization of TiO₂ Substrates by Monolayers of Porphyrin Heterodimers, *J. Phys. Chem. B*, 2000, **104**, 2371–2377.
- 10 A. J. Mozer, M. J. Griffith, G. Tsekouras, P. Wagner, G. G. Wallace, S. Mori, K. Sunahara, M. Miyashita, J. C. Earles, K. C. Gordon, L. Du, R. Katoh, A. Furube and D. L. Officer, Zn–Zn Porphyrin Dimer-Sensitized Solar Cells: Toward 3-D Light Harvesting, *J. Am. Chem. Soc.*, 2009, **131**, 15621–15623.
- 11 Y. Liu, H. Lin, J. T. Dy, K. Tamaki, J. Nakazaki, C. Nishiyama, S. Uchida, H. Segawa and J. Li, Kinetics versus Energetics in Dye-Sensitized Solar Cells Based on an Ethynyl-Linked Porphyrin Heterodimer, *J. Phys. Chem. C*, 2014, **118**, 1426–1435.
- 12 X. Zarate, E. Schott, T. Gomez and R. Arratia-Pérez, Theoretical Study of Sensitizer Candidates for Dye-Sensitized Solar Cells: Peripheral Substituted Dizinc Pyrazinoporphyrazine–Phthalocyanine Complexes, *J. Phys. Chem. A*, 2013, **117**, 430–438.
- 13 A. F. Nogueira, L. F. O. Furtado, A. L. B. Formiga, M. Nakamura, K. Araki and H. E. Toma, Sensitization of TiO₂ by Supramolecules Containing Zinc Porphyrins and Ruthenium–Polypyridyl Complexes, *Inorg. Chem.*, 2004, **43**, 396–398.
- 14 Z. S. Seddigi, S. A. Ahmed, S. Sardar and S. K. Pal, Ultrafast dynamics at the zinc phthalocyanine/zinc oxide nanohybrid interface for efficient solar light harvesting in the near red region, *Sol. Energy Mater. Sol. Cells*, 2015, **143**, 63–71.
- 15 J. P. Escalada, V. B. Arce, G. V. Porcal, M. A. Biasutti, S. Criado, N. A. García and D. O. Mártire, The effect of dichlorophen binding to silica nanoparticles on its photo-sensitized degradation in water, *Water Resour.*, 2014, **50**, 229–236.

- 16 V. Vaiano, O. Sacco, D. Sannino and P. Ciambelli, Photocatalytic removal of spiramycin from wastewater under visible light with N-doped TiO₂ photocatalysts, *Chem. Eng. J.*, 2015, **261**, 3–8.
- 17 N. Nasuha, B. H. Hameed and A. T. M. Din, Rejected tea as a potential low-cost adsorbent for the removal of methylene blue, *J. Hazard. Mater.*, 2010, **175**, 126–132.
- 18 B. Liu, L.-M. Liu, X.-F. Lang, H.-Y. Wang, X. W. Lou and E. S. Aydil, Doping high-surface-area mesoporous TiO₂ microspheres with carbonate for visible light hydrogen production, *Energy Environ. Sci.*, 2014, **7**, 2592–2597.
- 19 Z.-Q. Li, Y.-P. Que, L.-E. Mo, W.-C. Chen, Y. Ding, Y.-M. Ma, L. Jiang, L.-H. Hu and S.-Y. Dai, One-Pot Synthesis of Mesoporous TiO₂ Microspheres and Its Application for High-Efficiency Dye-Sensitized Solar Cells, *ACS Appl. Mater. Interfaces*, 2015, **7**, 10928–10934.
- 20 S. Sardar, P. Kar and S. K. Pal, The Impact of Central Metal Ions in Porphyrin Functionalized ZnO/TiO₂ for Enhanced Solar Energy Conversion, *J. Mater. NanoSci.*, 2014, **1**, 12–30.
- 21 S. Sardar, P. Kar, S. Sarkar, P. Lemmens and S. K. Pal, Interfacial carrier dynamics in PbS-ZnO light harvesting assemblies and their potential implication in photovoltaic/photocatalysis application, *Sol. Energy Mat. Sol. Cells*, 2015, **134**, 400–406.
- 22 S. Sardar, P. Kar, H. Remita, B. Liu, P. Lemmens, S. Kumar Pal and S. Ghosh, Enhanced Charge Separation and FRET at Heterojunctions between Semiconductor Nanoparticles and Conducting Polymer Nanofibers for Efficient Solar Light Harvesting, *Sci. Rep.*, 2015, **5**, 17313.
- 23 R. J. Baxter and P. Hu, Insight into why the Langmuir–Hinshelwood mechanism is generally preferred, *J. Chem. Phys.*, 2002, **116**, 4379–4381.
- 24 S. Sardar, S. Chaudhuri, P. Kar, S. Sarkar, P. Lemmens and S. K. Pal, Direct observation of key photoinduced dynamics in a potential nano-delivery vehicle of cancer drugs, *Phys. Chem. Chem. Phys.*, 2015, **17**, 166–177.
- 25 Z. S. Seddigi, S. A. Ahmed, S. Sardar and S. K. Pal, Carbonate Doping in TiO₂ Microsphere: The Key Parameter Influencing Others for Efficient Dye Sensitized Solar Cell, *Sci. Rep.*, 2016, **6**, 23209.
- 26 H. C. Junqueira, D. Severino, L. G. Dias, M. S. Gugliotti and M. S. Baptista, Modulation of methylene blue photochemical properties based on adsorption at aqueous micelle interfaces, *Phys. Chem. Chem. Phys.*, 2002, **4**, 2320–2328.
- 27 C. Yogi, K. Kojima, N. Wada, H. Tokumoto, T. Takai, T. Mizoguchi and H. Tamiaki, Photocatalytic degradation of methylene blue by TiO₂ film and Au particles-TiO₂ composite film, *Thin Solid Films*, 2008, **516**, 5881–5884.
- 28 A. Mills and J. Wang, Photobleaching of methylene blue sensitised by TiO₂: an ambiguous system?, *J. Photochem. Photobiol., A*, 1999, **127**, 123–134.